Supporting Information

Huitema et al. 10.1073/pnas.1214231110

SI Materials and Methods

Alizarin Red/Alcian Blue Skeletal Staining. Skeletal staining was performed as described previously (1, 2), and specimens were stored in 70% (vol/vol) glycerol at 4 °C. In vivo skeletal staining was performed with 0.001% calcein or 0.05% alizarin red in E3 medium for 5–10 min and subsequent extensive washes with E3 medium.

Meiotic Mapping and Sequencing. Bioinformatic construction of the genomic region surrounding the *no bone* (*nob*)^{hu3718} and *dragonfish* (*dgf*)^{hu4581} genes was performed using Ensembl database Zv6 (http://genome.ucsc.edu/cgi-bin/hgGateway?hgsid=312908511&clade=vertebrate&org=Zebrafish&db=danRer6) for *nob*^{hu3718} and Zv9 (www.ensembl.org/Danio_rerio/Info/Index?db=core) for *dgf*^{hu4581}. Meiotic mapping of the *nob*^{hu3718} and *dgf*^{hu4581} mutations was performed using standard simple sequence-length polymorphisms and single-nucleotide polymorphisms.

For sequencing of candidate genes, coding exons of the respective gene were amplified separately from mutant and wild-type embryos and sequenced on both strands. The Leu155>stop mutation in nobhu3718 was confirmed with primers nob3718-ex3-fw and nobhu3718ex3-rev. The Thr80>Ala mutation of nobhu5310 was confirmed with primers nobhu5310 -ex1-fw and nobhu5310-ex1-rev. The splice acceptor mutation of dgfhu4581 was confirmed with primers dgfGfw and dgfGrev. Sequencing of the cDNA (primers dgfCfw and dgfCrv) revealed a frameshift leading to a predicted stop codon after a further 23 amino acids. No alternative transcripts could be detected by RT-PCR. The Arg427>stop mutation of dgfsa156 was confirmed with primers saGfw and saGrv. All primer sequences are shown in Table S1. PCR conditions are available upon request.

For all experiments, we have used the *nob*^{hu3718} and *dgf*^{hu4581} alleles, unless stated otherwise.

Whole-Mount in Situ Hybridization and Immunohistochemistry. All in situ hybridizations were performed at least twice as previously described (1, 3) and embryos were subsequently genotyped. Previously described probes were osterix and col10a1 (1). Probes generated for sox9a and ectonucleoside triphosphate/diphosphohydrolase 5 (entpd5) were transcribed from the 5′ part of the respective cDNA (for primers sequences, see Table S1).

Immunohistochemistry was essentially done as described (4). Embryos were fixed for 1 h in 4% paraformaldehyde and stored in methanol. Embryos were rehydrated, blocked in PBS with 5% lamb serum, and incubated with 1:500 anti–phospho-Histone H3 (Millipore) and anti-collagen II (1:500; Developmental Studies Hybridoma Bank) overnight at 4 °C. Embryos were washed extensively and then incubated in Alexa Fluor secondary antibodies (diluted 1:500 in blocking solution; Molecular Probes) for 3 h at room temperature. Embryos were washed extensively in the dark and mounted for analysis.

cDNA Rescue Experiments. TRIzol reagent (Invitrogen) was used to extract RNA from 6-dpf (days postfertilization) embryos, and mouse RNA was extracted from cultured KS483 cells (5). First-strand cDNA was generated using either cloning *entpd5* R (fish) primers or cloning Entpd5 R (mouse) primers (Table S1). Second-strand cDNA was synthesized using M-MLV reverse transcriptase (Promega) according to the manufacturer's protocol. Zebrafish entpd5 cDNA was cloned into PCS2+ and into pBluescript containing the osterix promoter (1). One-cell–stage embryos derived from *nob*^{hu3718} carrier fish were injected with plasmid DNA in a maximum volume of 2 nL. Alizarin red/alcian blue staining was carried out at 6 dpf. Only injected embryos with normal size, apparently normal cartilage, and without tissue malformations or general edema or apparent toxic defects were included for analysis. Each rescue experiment was performed three independent times. In total, we scored 490 siblings/131 mutant embryos injected with 100 pg cmv:entpd5; 329 siblings/106 mutants injected with 100 pg osterix:entpd5; 500 siblings/166 mutants with 100 pg cmv:Entpd5 (murine cDNA); 151 siblings/63 mutants with 100 pg cmv:nobhu5310; and 481 sibling/129 mutants with 25 pg kdr-l:entpd5 cDNA.

Animal Procedures. All zebrafish strains were maintained at the Hubrecht Institute using standard husbandry conditions. Animal experiments were approved by the Animal Experimentation Committee of the Royal Netherlands Academy of Arts and Sciences.

Mutagenesis and Screening. N-Ethylnitrosourea mutagenesis and screening were performed as previously described (6, 7). Embryos were grown in E3 medium until 8 dpf and subsequently fixed for skeletal staining (alizarin red/alcian blue) as described below.

Embryo Media. Embryos were kept in E3 embryo medium (5 mM NaCl, 0.17 mM KCl, 0.33 mM $CaCl_2$, 0.33 mM $MgSO_4$) at 28 °C. For phosphate rescue experiments, embryos were kept in PBS medium (137 mM NaCl, 2.7 mM KCl, 9 mM $CaCl_2$, 0.5 mM $MgCl_2$, 8 mM $Na_2HPO_40.2H_2O$, 1.47 mM KH_2PO_4, pH 7.4). For calcium rescue experiments, embryos were kept in E3 embryo medium + 10 mM $CaCl_2$.

For anesthesia, a 0.2% solution of 3-aminobenzoic acid ethyl ester (Sigma) containing Tris buffer (pH 7) was used (8).

Transgenic Lines. Transgenic lines were generated as described by Bussmann and Schulte-Merker (9). Fluorophores were recombined into the ATG site of the *entpd5* gene (BAC clone CH211-202H12). Sequences of primers used are available on request.

BAC Rescue Experiment. BAC clone DKEY-173L2 used for a stable rescue of *dgf*^{hu4581} contains all exons and untranslated regions of the *enpp1* gene and 87 kb of the upstream regulatory region. The first exon of the two-exon gene *kcnk3*, which is also present on the BAC, was replaced through BAC recombineering with a cassette containing YFP under a CMV promoter (Fig. 3*F*), effectively eliminating gene function. Transgenic lines were generated as described (9). Carriers passed on the transgene to ∼50% of their offspring, indicative of a single BAC integration event. Upon crossing *dgf*$^{+/-}$, *enpp1*-BAC^{+} with *dgf*$^{+/-}$ individuals, we observed a mutant phenotype in less than 1/8 (9.4%) of the embryos at 8 dpf. None of the embryos with a mutant phenotype tested positive for integration of the BAC construct by PCR (16/16). Primer locations are indicated in Fig. 3*F* (small arrows fw and rv); sequences are DgfBacIntfw/DgfBacIntrv in Table S1. To test for the presence of rescued embryos, we performed genotyping using an SNP marker (CASCAD 039178) (10) linked to the mutant *dgf* allele but situated outside the genomic region covered by the BAC. This was necessary, because sequencing of the *dgf* locus itself is not informative due to the presence of three copies of *enpp1* in the genome of transgenic fish. Within the transgenic population, we could find approximately a quarter of embryos (6/23) with the variant of the SNP linked to the mutant *dgf* allele. These embryos were phenotypically indistinguishable from heterozygous or wild-type embryos of the same clutch (Fig. 4*A*, *Lower*). This shows that a BAC containing *enpp1* is sufficient to

rescue the *dgf* phenotype, and therefore confirms causality of the genetic lesion identified in the *dgf* mutant line.

Microarray. Analysis of the microarray data is available (Gene Expression Omnibus accession no. GSE35737; www.ncbi.nlm.nih.gov/geo/query/acc.cgi?token=npqhtqgomsaakvy&acc=GSE35737).

Quantitative Real-Time PCR. *Nob* mutant and sibling embryos were separated at 6 dpf by in vivo skeletal (alizarin red) staining and allowed to recover for 24 hpf at 28 °C. For total RNA isolation from 7-dpf embryos, a maximum of $n = 40$ *nob* mutant and sibling embryos per clutch was homogenized by shredding in 600 μL of RTL lysis buffer (Qiagen RNeasy Kit) containing 10% β-mercaptoethanol. One volume of 70% ethanol was added and the homogenate was loaded onto a column for total RNA isolation according to the manufacturer's protocol, followed by DNaseI (Promega) treatment. RNA quality and concentration were determined using a NanoDrop spectrophotometer (Thermo Scientific) and verified by gel electrophoresis. cDNA was synthesized from total RNA (1–5 μg) with random hexamers (Integrated DNA Technologies) using reverse transcriptase M-MLV (Promega). Primer sets were designed using Primer3 (http://frodo.wi.mit.edu/primer3) with an optimal product size of 110–200 bp and, where possible, spanning two exons to avoid genomic contamination (for primer sequences, see Table S1). PCR efficiency and optimal melting temperatures were determined per primer set, and the specificity was verified by gel electrophoresis using standard real-time PCR on zebrafish cDNA. Quantitative PCR was performed using the MyiQ Single-Color Real-Time PCR Detection System and software (Bio-Rad). Each reaction contained 12.5 μL SYBR Green fluorescent label (Bio-Rad), 3 μL 1.5 μM primer mix, 4.5 μL MQ, and 5 μL cDNA (10 ng/μL). Cycling conditions were 95 °C for 3 min; 40 cycles of 95 °C for 10 s and the optimal primer temperature for 45 s; 95 °C for 1 min; and finally 65 °C for 1 min. All reactions were performed in triplicate on cDNA isolated from at least three different clutches of pooled 7-dpf *nob* mutant and sibling embryos. Cycle threshhold values were corrected for the *ef1a* housekeeping gene. *Nob* mutant cDNA concentrations were calculated in arbitrary units compared with the sibling average, and are represented as the fold change with the sibling value set to 1. For data analysis, groups were compared by paired Student's *t* test.

Imaging. Embryos were mounted in 0.5% low-melting-point agarose in a culture dish with a coverslip replacing the bottom. Imaging was performed with an SP2 confocal microscope (Leica Microsystems) using a 10× or 20× objective with digital zoom. Usually, z stacks spanning ∼5 μm were captured and then flattened by maximum projection in ImageJ (National Institutes of Health).

1. Spoorendonk KM, et al. (2008) Retinoic acid and Cyp26b1 are critical regulators of osteogenesis in the axial skeleton. *Development* 135(22):3765–3774.
2. Walker MB, Kimmel CB (2007) A two-color acid-free cartilage and bone stain for zebrafish larvae. *Biotech Histochem* 82(1):23–28.
3. Schulte-Merker S (2002) Looking at embryos. *Zebrafish: A Practical Approach*, eds Nüsslein-Volhard C, Dahm R (Oxford Univ Press, New York), pp 41–43.
4. Hammond CL, Schulte-Merker S (2009) Two populations of endochondral osteoblasts with differential sensitivity to Hedgehog signalling. *Development* 136(23): 3991–4000.
5. Yamashita T, et al. (1996) Subcloning of three osteoblastic cell lines with distinct differentiation phenotypes from the mouse osteoblastic cell line KS-4. *Bone* 19(5): 429–436.
6. Spoorendonk KM, Hammond CL, Huitema LFA, Vanoevelen J, Schulte-Merker S (2010) Zebrafish as a unique model system in bone research: The power of genetics and in vivo imaging. *J Appl Ichthyol* 26(2):219–224.
7. Haffter P, et al. (1996) The identification of genes with unique and essential functions in the development of the zebrafish, *Danio rerio*. *Development* 123:1–36.
8. Brand M, Granato M, Nüsslein-Volhard C (2002) Keeping and raising zebrafish. *Zebrafish: A Practical Approach*, eds Nüsslein-Volhard C, Dahm R (Oxford Univ Press, New York), pp 7–37.
9. Bussmann J, Schulte-Merker S (2011) Rapid BAC selection for tol2-mediated transgenesis in zebrafish. *Development* 138(19):4327–4332.
10. Guryev V, Berezikov E, Cuppen E (2005) CASCAD: A database of annotated candidate single nucleotide polymorphisms associated with expressed sequences. *BMC Genomics* 6:10.

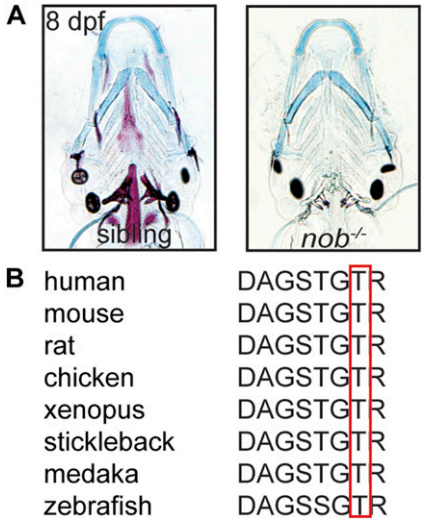

Fig. S1. (*A*) Alcian blue staining is unaltered in *nob* mutants versus siblings. The images are similar to the ones presented in Fig. 1*A*, but taken with higher contrast settings to allow an appreciation of normal chondrocyte morphology in mutant embryos. (*B*) Multiple sequence alignment of Entpd5 proteins demonstrating the conserved nature of zebrafish Thr80 in the first apyrase domain.

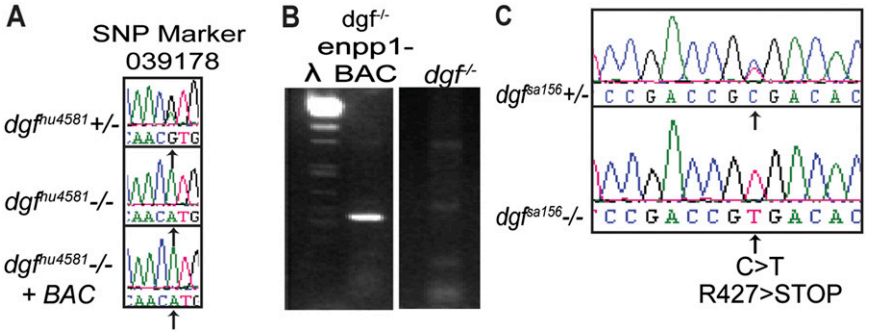

Fig. S2. *dgf*$^{-/-}$ mutant embryos can be rescued by transgenic insertion of a BAC containing the *enpp1* gene, and *dgfsa156* encodes a mutation in *enpp1*. (*A*) BAC-rescued embryos exhibit a wild-type phenotype (shown in Fig. 3*A*). The SNP variant (arrow) is linked to the *dgf* mutation (sequence, *Middle*). (*B*) PCR indicating the presence of the enpp1 BAC in rescued *dgf*$^{-/-}$ embryos and its absence in nonrescued *dgf*$^{-/-}$ embryos. (*C*) Sequencing of the *dgfsa156* allele, kindly provided by The Sanger Center, reveals an Arg427>stop in the *enpp1* gene.

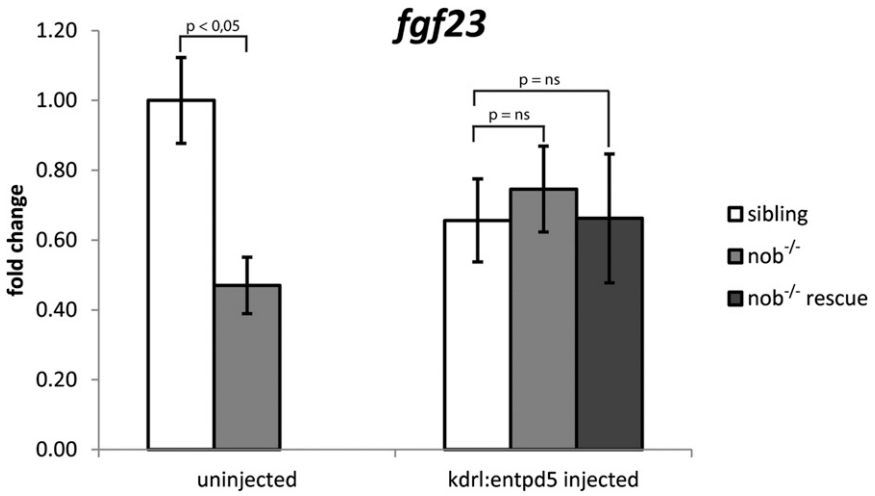

Fig. S3. Quantitative real-time PCR for *fgf23* levels in 7-dpf embryos. (*Left*) Uninjected siblings vs. mutants are depicted. (*Right*) Embryos were injected with a *kdrl:entpd5* plasmid, stained with alizarin red, and categorized into siblings (normal mineralization), mutants without any signs of rescue (compare Fig. 2*J*, *Center*), and mutants with partial rescue (compare Fig. 2*J*, *Right*). Transcript levels were normalized to the level in uninjected siblings.

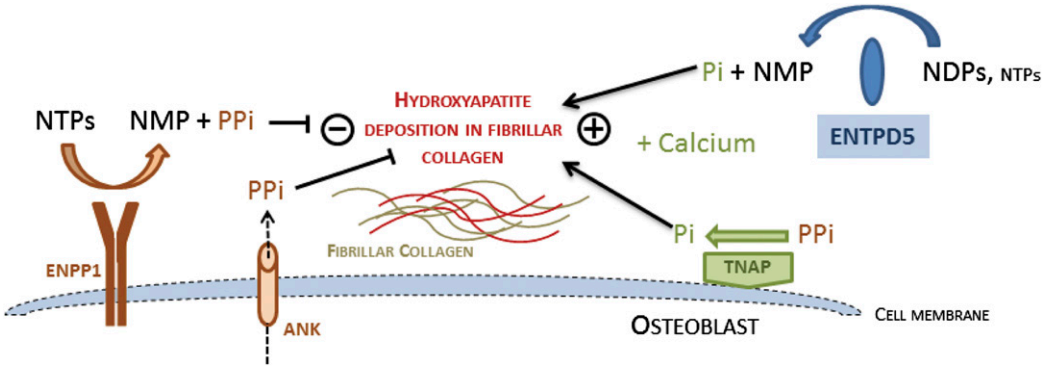

Fig. S4. *Entpd5* encodes an essential determinant of extracellular phosphate and bone mineralization. A graphical abstract depicts the interaction of Entpd5, Enpp1, and other factors that regulate extracellular phosphate and pyrophosphate levels. Enpp1 activity leads to the generation of pyrophosphate, and in addition there is transport of pyrophosphate via the transmembrane channel ANK. Pyrophosphate inhibits the biomineralization process that occurs on the fibrillar collagen matrix (osteoid). This negative effect is counterbalanced by tissue-nonspecific alkaline phosphatase (TNAP)-mediated hydrolysis of pyrophosphate. This process generates free phosphate. Our data indicate that ENTPD5 is an essential contributor in generating sufficiently high levels of free phosphate necessary for proper mineralization. Biochemical studies suggest that this is achieved by hydrolyzing phosphate from nucleotide diphosphates (NDPs) (and, to a lower extent, also NTPs). Please note that TNAP has been shown in mammals to be a key component for mineralization to occur. The respective contributions of TNAP in teleosts remain to be established, as does the role of Entpd5 in mammals. In the case of the *dgf* mutant embryos, Enpp1 activity is absent, and hence there is less pyrophosphate available and the phosphate/pyrophosphate balance is shifted toward higher phosphate levels, resulting in more mineralization. In *nob* mutants, phosphate levels are lower, tipping the balance in favor of pyrophosphate, leading to a failure to mineralize. NMP, nucleotide monophosphate.

Table S1. Primer sequences

Primer name	Sequence (5′–3′)
sox9a.fw	CAGACACCAGCAGACAACAAA
sox9a.rev	CGTTCTTCACCGACTTCCTC
col1a2.fw	GACATTGGCCCAGTCTGTTT
col1a2.rev	GGATTATCAGGGGGACCTGT
nobhu3718-ex3-fw	AGACAATCCCCAAAGAGCAA
nobhu3718-ex3-rev	GCTCCAGACAGCCTCAAAAC
nobhu5310-ex1-fw	TTAACAAGACCGGGCAAAAG
nobhu5310-ex1-rev	GAGGCATGGATGTGAGTCAG
dgfGfw	GTTGCATTTGCCTGAAGGAG
dgfGrev	CAGAAATTTTCCCCTAACTAAGCA
dgfCfw	TCCCGCTGGGTTTTCTAAAT
dgfCrv	AACATCCCAATCAGCCTGTC
saGfw	GCGTGCATATCAAACACACA
saGrv	GATGTGTGTCAAGTTAAATCTGTGC
dgfRTfw1	TCCCGCTGGGTTTTCTAAAT
dgfRTrv1	AACATCCCAATCAGCCTGTC
dgfRTfw2	TCCCGCTGGGTTTTCTAAAT
dgfRTrv2	AACATCCCAATCAGCCTGTC
dgfRTfw3	TCCCGCTGGGTTTTCTAAAT
dgfRTrv3	AACATCCCAATCAGCCTGTC
DgfBacIntfw	CGTTGGCTACCCGTGATATT
DgfBacIntrv	TGCTGAAGGAACAGCTCAGT
probe.entpd5.fish.fw	TTTTTGCCGGGTACTTTCTG
probe.entpd5.fish.rev	GAGTTGAACCTCCACCCAAA
Cloning *entpd5* R (fish)	TCAGCAAGTACCCTGAATGCTG
Cloning Entpd5 R (mouse)	CACCCACCAAGTGGTTAGGA
qPCR.entpd5.fw	ATATGCCTGAAAAGGGTGGA
qPCR.entpd5.rev	TACTTCTTTGACCTCATTCAGCAG
qPCR.fgf23.fw	CGGGGCTCATACAGTGTAATC
qPCR.fgf23.rev	TCCAACAGTTTGTGGTGGAA
qPCR.phex.fw	CCGTCATCACGGTATCACAA
qPCR.phex.rev	TCTGAGCCATGGGTAAATCC
qPCR.phospho1.fw	TGAAAACAGGAGCAGCTGTAAA
qPCR.phospho1.rev	GGGGCTGGAGATCTGCTT
qPCR.npt2a.fw	TCATCCAGAAGGTCATCAACA
qPCR.npt2a.rev	ATCACACCCAGGCCAATG

Primer sets were designed using Primer3 (http://frodo.wi.mit.edu/primer3). fw, forward; rev, reverse.